Physica Scripta. Vol. 63, 104–107, 2001

Branching Fractions for the $5s^25p^2 - 5s^25p6s$ Supermultiplet in the Sn Isoelectronic Sequence

Lorenzo J. Curtis*

Department of Physics and Astronomy, University of Toledo, Toledo, Ohio 43606, USA

Received July 3, 2000; accepted August 14, 2000

PACS REF: 32.70.Cs, 32.70.Fw

Abstract

Recent studies of the Si and Ge isoelectronic sequences have shown that branching fractions within the ns^2np^2–$ns^2np(n+1)s$ supermultiplets are accurately described by a semiempirical model that uses spectroscopic energy level data to characterize intermediate coupling. It was also recently shown that a similar model applied to alkaline-earthlike ns^2–$nsnp$ transitions can be advantageously generalized to include the effects of spin-other-orbit interaction and differences between the singlet and triplet radial wave functions. These two formalisms are combined, extended, and applied here to obtain a predictive systematization of branching fractions for the $5s^25p^2$–$5s^25p6s$ supermultiplet of the ions Sn I–Cs VI in the Sn sequence.

1. Introduction

Although lifetime measurement data now exist that extend through many stages of ionization along isoelectronic sequences, the use of this these data to specify transition probability rates and oscillator strengths is hindered by the nearly total lack of branching fraction data for multiply charged ions [1,2]. Factors contributing to this deficiency include the difficulties inherent in the intensity calibration of the detection apparatus applicable to sources of highly ionized atomic spectra, and to the lack of intensity calibration standards in the ultraviolet region where these spectra occur. As one approach to this problem, studies have been made of several supermultiplets between polyads dominated by a single configuration. In such cases, intermediate coupling amplitudes obtained from spectroscopic data can be used to accurately predict relative intensities.

It has been shown [3] that transitions of the form ns^2np^2–$ns^2np(n+1)s$ in neutral Si I and Ge I are virtually free of configuration interaction, and can thus be semiempirically specified using spectroscopically determined singlet-triplet mixing angles. These successes motivated the extension [4] of this method to the isoelectronic counterparts P II - Ar V in the Si sequence and As II - Br IV in the Ge sequence. Similar studies have also been carried out [5] for Pb I and Bi II in the Pb sequence. In addition, in a recent study of the ns^2–$nsnp$ and $nsnp$–$nsnd$ transitions in Ga II, In II and Tl II, it was shown [6] that this singlet-triplet mixing angle formulation can be extended to include the effects of both spin-other-orbit interaction and differences between the singlet and triplet radial wave functions. This is accomplished by an extension of the number of parameters, allowing the diagonal and off-diagonal magnetic energies to be varied independently in their determination from the spectroscopic data. Reported here is the combination, extension, and application of these methods to the prediction of branching fractions for the ions Sn I–Cs VI in the Sn isoelectronic sequence.

2. Calculational Formulation

In the standard *LS* formulation, the energy level separations of the levels are specified [7] from the direct and exchange Slater parameters and spin-orbit energies: F_2, ζ_{pp} for a p^2 configuration; G_1, ζ_p for an sp configuration. In the *LS* representation F_2 and G_1 have only diagonal elements, whereas ζ_{pp} and ζ_p have both diagonal and off-diagonal values.

As discussed in Ref. [6], this formulation has been generalized to include spin-other-orbit interaction and differences between the singlet and triplet radial wave functions. Already in 1932, Wolfe [7,8] pointed out that the effects of spin-own-orbit and spin-other-orbit interactions add on the diagonal and subtract on the off-diagonal. In 1939 King and Van Vleck [9] expanded this approach, suggesting that small differences between the (non-relativistically equal) singlet and triplet radial wave functions could also lead to differences between the diagonal and off-diagonal magnetic energy parameters. Thus an improved parameterization is obtained by allowing the diagonal and off-diagonal values for ζ_p (henceforth denoted as μ_1 and μ_2 respectively) to be treated as independent parameters, separately determined from spectroscopic data. This extends the number of fitting parameters to three, hence the data reduction becomes a simple one-to-one remapping of the three independent energy level splittings.

In the present study a similar generalization is made for the p^2 configuration. In this case the quantity ζ_{pp} also occurs on the diagonal and the off-diagonal, but on the latter it couples both the $J = 2$ and the $J = 0$ levels. To characterize this, three magnetic parameters were introduced (henceforth denoted by ζ_1 on the diagonal and ζ_0 and ζ_2 for the $J = 0$ and 2 off-diagonal elements). This extends the number of fitting parameters to four, so again this data reduction becomes a simple one-to-one remapping of the four independent energy level splittings.

In terms of these parametrizations, the levels (denoted here by their nominal *LS* symbols, with spin-mixed cases indicated by primes) can be written for the p^2 configuration as

$$^1D_2', {}^3P_2' = E_0 - 2F_2 + \zeta_1/4 \pm \Delta_2, \quad (1)$$

$$^3P_1 = E_0 - 5F_2 - \zeta_1/2, \quad (2)$$

* e-mail: ljc@physics.utoledo.edu

$$^1S'_0, ^3P'_0 = E_0 + 5F_2/2 - \zeta_1/2 \pm \Delta_0 \quad (3)$$

where

$$\Delta_2 \equiv \sqrt{(3F_2 - \zeta_1/4)^2 + \zeta_2^2/2}, \quad (4)$$

$$\Delta_0 \equiv \sqrt{(15F_2/2 + \zeta_1/2)^2 + 2\zeta_0^2} \quad (5)$$

and for the sp configuration by [6]

$$^3P^o_2 = E_1 - G_1 + \mu_1/2, \quad (6)$$

$$^1P^{o\prime}_1, ^3P^{o\prime}_1 = E_1 - \mu_1/4 \pm \Delta_1, \quad (7)$$

$$^3P^o_0 = E_1 - G_1 - \mu_1 \quad (8)$$

where

$$\Delta_1 \equiv \sqrt{(G_1 + \mu_1/4)^2 + \mu_2^2/2}. \quad (9)$$

The quantities E_0 and E_1 provide an overall baseline that does not enter in the determination of the intermediate coupling amplitudes. Given experimental energy level data, the quantities F_2, ζ_1, ζ_2, ζ_0 and G_1, μ_1, μ_2 can be deduced by simple algebraic manipulations [10]. It also has been shown [10] that the intermediate coupling amplitudes can be formulated in terms of the singlet-triplet mixing angles θ_0, θ_2 (for the J=0 and 2 levels of the p^2 configuration) and θ_1 (for the J=1 levels of the sp configuration, given by

$$\cot 2\theta_0 = (15F_2 + \zeta_1)/\sqrt{8}\zeta_0, \quad (10)$$

$$\cot 2\theta_2 = (12F_2 - \zeta_1)/\sqrt{8}\zeta_2, \quad (11)$$

$$\cot 2\theta_1 = (4G_1 + \mu_1)/\sqrt{8}\mu_2. \quad (12)$$

These singlet-triplet mixing angles can be used to specify relative transition rates using LS values for the transition elements [6,7].

3. Data Reduction

The spectroscopic data base used is given in Table I, taken from the following sources: Sn I [11,12], Sb II [13], Te III [14], I IV [15], Xe V [16], Cs VI [17]. These data for the energy level splittings were mapped into their equivalent Slater and magnetic energy parameter spaces using Eqs. (1–9), and those values are listed in Table II. The fact that the fitted values of the ζ_k and μ_k parameters are very close to each other for various values of k indicates that configuration interaction is weak, and that the system is accurately represented by the effective values of the empirical parameters that occur in this quasi single configuration model representation.

The values of the singlet-triplet mixing angles were deduced from the fitted parameters using Eqs. (10–12), and are also listed in Table II. It has been observed that when the mixing angle data are studied as the cotangents of the double angles (as they occur in Eqs. (10–12)), they have

Table I. *Energy level data base (in cm^{-1}).*

	Level	Sn I[a]	Sb II[b]	Te III[c]	I IV[d]	Xe V[e]	Cs VI[f]
$5s^25p^2$	$^3P'_0$	0	0	0	0	0	0
	$^3P_1$	1 691.806	3 054.6	4 756.5	6 828.2	9 320.	12 176.0
	$^3P'_2$	3 427.673	5 658.2	8 166.9	10 981.5	14 150.	17 628.2
	$^1D'_2$	8 612.955	12 789.8	17 359.1	22 531.9	28 440.	35 061.4
	$^1S'_0$	17 162.6[g]	23 905.5	31 420.0	37 177.2	44 580.	52 410.3
$5s^25p6s$	$^3P^{o\prime}_0$	34 640.76	69 137.3	107 468.5	149 049.4	(194 000)[h]	242 213.3
	$^3P^{o\prime}_1$	34 914.28	69 535.7	107 723.4	150 085.8	(195 000)[h]	243 719.2
	$^3P^{o\prime}_2$	38 628.88	75 274.5	114 215.1	160 836.9	209 100.	260 952.0
	$^1P^{o\prime}_1$	39 257.05	75 898.9	115 420.3	161 382.3	213 135.	264 226.7

[a] Brown *et al.* [11].
[b] Arcimowicz *et al.* [13].
[c] Crooker and Joshi [14].
[d] Tauheed *et al.* [15].
[e] Pinnington *et al.* [16].
[f] Tauheed *et al.* [17].
[g] Moore [12].
[h] Interpolated value.

Table II. *Empirical singlet-triplet mixing angles (as double angle cotangents) and effective Slater and magnetic energy parameters (in cm^{-1}).*

Z	Ion	cot $2\theta_0$	cot $2\theta_2$	cot $2\theta_1$	F_2	ζ_1	ζ_2	ζ_0	G_1	μ_1	μ_2
50	Sn I	–2.435	1.691	0.599	919	2 097	1 867	2 305	451	2 659	2 635
51	Sb II	–1.952	1.148	0.550	1 186	3 480	3 312	3 853	511	4 091	3 942
52	Te III	–1.621	0.954	0.550	1 460	4 833	4 702	5 833	730	4 498	4 769
53	I IV	–1.433	0.598	0.559	1 568	6 966	7 010	7 523	791	7 858	6 973
54	Xe V	–1.267	0.449	0.668	1 729	9 049	9 219	9 767	2 518	10 067	10 066
55	Cs VI	–1.145	0.334	0.638	1 871	11 410	11 693	12 192	2 390	12 493	12 226

a nearly linear behavior when plotted *vs* the reciprocal of an appropriate effective charge, here $1/(Z\text{-}47)$. A plot made for this system is shown in Fig. 1. This exposition can be very useful for interpolation, extrapolation, and identifying inconsistencies in the observations. Notice that the value of $\cot 2\theta_2$ is well off the trend for Te III, indicating a value near 0.82, rather than 0.954 as obtained from the observations (cf. Table II). This motivates a re-examination of the energies of the $J = 2$ levels in the ground configuration of Te III.

The mixing angles so obtained were then used to compute the relative transition rates, and therefore the branching fractions, using the relationships presented in Ref. [3].

4. Results

The results applied to Sn I and Sb II are given in Table III, together with the theoretical predictions of Bierón *et al.* [18] (selecting their recommended MCDM-EAL calculation in Babushkin gauge). For the case of Sn I, experimental values are also available, and a sampling [19–21] are listed in Table III for comparison. (The tabulation of the measurements of Lotrian *et al.* [19] is here corrected for a transcription error made in the tabulation presented in Ref. [3]). The semiempirical values reported here are in good general agreement with the *ab initio* theoretical calculations. Agreement between semiempirical and experimental values is also satisfactory to within the variations among the measurements.

On the basis of this agreement between semiempirical, experimental, and theoretical values, the analysis was extended to the multiply charged ions Te III, I IV, Xe V and Cs VI in this isoelectronic sequence. The results of these calculations are presented in Table IV.

5. Conclusions

It is observed, both empirically and theoretically, that the nominally labelled polyads $5s^25p^2$ and $5s^25s6s$ are well des-

Table III. *Wavelengths and semiempirical, theoretical and experimental branching fractions for $5s^25p^2$–$5s^25p6s$ transitions in Sn I and Sb II.*

	Sn I						Sb II		
		BF(%)						BF(%)	
Transition	λ(Å)[a]	SE[b]	B[c]	L[d]	CB[e]	M[f]	λ(Å)[a]	SE[b]	B[c]
$^3P'_0 \leftarrow {}^3P^{o\prime}_1$	2863.32	32.3	28.9	27	37	40	1438.11	30.2	38.4
$^3P_1 \leftarrow$	3009.13	17.5	20.9	17	27	28	1504.19	16.1	23.8
$^3P'_2 \leftarrow$	3175.03	39.7	41.8	39	22	22	1565.50	43.4	31.9
$^1D'_2 \leftarrow$	3801.01	10.0	8.2	17	14	11	1762.24	9.5	5.7
$^1S'_0 \leftarrow$	5631.71	0.5	0.2	–	0.3	0.2	2190.85	0.8	0.2
$^3P_1 \leftarrow {}^3P^o_2$	2706.50	28.3	25.3	22	30	32	1384.66	27.8	14.8
$^3P'_2 \leftarrow$	2839.98	68.5	72.1	71	64	63	1436.45	65.5	48.4
$^1D'_2 \leftarrow$	3330.61	3.2	2.6	7	6	5	1600.39	6.6	36.8
$^3P'_0 \leftarrow {}^1P^{o\prime}_1$	2546.55	4.2	3.6	8	21	25	1317.54	3.0	1.6
$^3P_1 \leftarrow$	2661.24	6.8	3.6	4	13	14	1372.79	6.0	1.8
$^3P'_2 \leftarrow$	2790.18	0.01	0.8	–	–	–	1423.68	0.6	0.5
$^1D'_2 \leftarrow$	3262.33	82.2	84.3	88	60	57	1584.56	80.2	84.7
$^1S'_0 \leftarrow$	4624.75	6.8	7.7	–	6	4	1923.32	10.2	11.5

[a] Air wavelengths for $\lambda > 2000$ Å.
[b] Semiempirical, this work.
[c] Bieroń *et al.* [18], theoretical (MCDM-EAL with Babushkin gauge).
[d] Lotrian *et al.* [19], arc emission.
[e] Corliss and Bozman [20], arc emission.
[f] Meggers *et al.* [21], arc emission.

Table IV. *Wavelengths and semiempirical branching fractions for $5s^25p^2$-$5s^25p6s$ transitions in multiply charged ions of the Sn sequence.*

	Te III		I IV		Xe V		Cs VI	
Transition	λ(Å)	BF(%)	λ(Å)	BF(%)	λ(Å)	BF(%)	λ(Å)	BF(%)
$^3P'_0 \leftarrow {}^3P^{o\prime}_1$	928.30	30.1	666.29	30.0	512.82	31.1	410.31	31.0
$^3P_1 \leftarrow$	971.19	15.6	698.04	15.3	538.56	16.1	431.89	15.6
$^3P'_2 \leftarrow$	1004.45	45.1	718.89	49.0	552.94	50.0	442.30	51.2
$^1D'_2 \leftarrow$	1106.63	8.5	783.98	5.0	600.38	2.4	479.25	1.8
$^1S'_0 \leftarrow$	1310.56	0.7	885.67	0.7	664.81	0.4	522.72	0.3
$^3P_1 \leftarrow {}^3P^o_2$	913.59	27.6	649.31	27.6	500.55	27.6	401.97	27.7
$^3P'_2 \leftarrow$	942.97	63.6	667.31	57.8	512.95	54.3	410.98	51.1
$^1D'_2 \leftarrow$	1032.46	8.9	723.04	14.6	553.53	18.1	442.69	21.2
$^3P'_0 \leftarrow {}^1P^{o\prime}_1$	866.40	2.1	619.65	1.5	469.19	0.7	378.46	0.6
$^3P_1 \leftarrow$	903.64	5.6	647.02	5.2	490.64	4.3	396.75	4.4
$^3P'_2 \leftarrow$	932.37	1.4	664.89	5.2	502.55	9.4	405.52	11.9
$^1D'_2 \leftarrow$	1019.77	79.2	720.20	74.8	541.43	71.6	436.37	68.6
$^1S'_0 \leftarrow$	1190.47	11.7	805.12	13.3	593.28	14.1	472.11	14.6

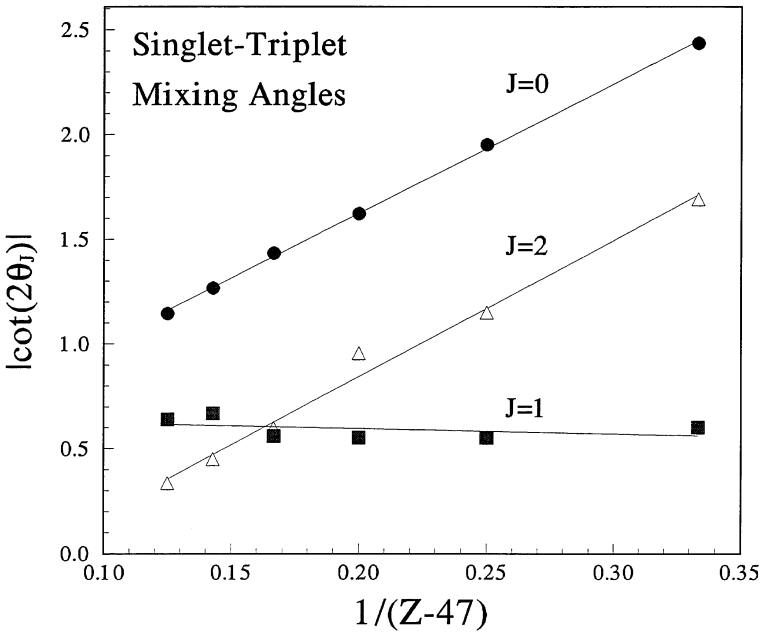

Fig. 1. Isoelectronic plot of the magnitude of $\cot 2\theta_0$, $\cot 2\theta_2$ and $\cot 2\theta_1$ *vs* the reciprocal of the effective screened charge. The symbols denote the values taken from Table II, and are connected by straight line fits to the data.

cribed by a parametrization based on their dominant configurations, and exhibit only weak effects of configuration interaction. In addition, theoretical calculations indicate that no strong cancellation effects occur in their radial transition integrals. Thus it can be concluded that the branching fractions obtained here from empirical values for the intermediate coupling amplitudes should be quite reliable.

Given accurate lifetime measurements of the upper levels, these branching fractions can be utilized to obtain transition probability rates and oscillator strength values for use in plasma modelling and abundance determinations. Moreover, these branching fractions also provide relative intensity calibration standards in the ultraviolet spectral region, which could be used to deduce relative intensities from spectra obtained from light sources involving fast ion beam excitation and ion trap studies. It is also clear from Fig. 1 that these mixing angles can be reliably extrapolated to higher values of Z, where no spectroscopic data presently exist. These extrapolated mixing angles could be used to predict the branching ratios before the spectral lines are known, and used to identify and classify the spectra that are ultimately measured.

Acknowledgement

This work was supported by the U.S. Department of Energy, Office of Basic Energy Sciences, Division of Chemical Sciences, under Grant number DE-FG02-94ER14461.

References

1. Curtis, L. J., "Precision Oscillator Strength and Lifetime Measurements," in "Atomic, Molecular & Optical Physics Handbook", (Edited by G. W. F. Drake), (AIP Press, 1996), pp. 206–212.
2. Curtis, L. J. and Martinson, I., "Lifetimes of Excited States in Highly Charged Ions", in "Atomic Physics with Heavy Ions", (Edited by H. F. Beyer and V. P. Shevelko), (Springer-Verlag, Berlin/Heidelberg, 1999), pp. 197–218.
3. Curtis, L. J., J. Phys. B **31**, L769 (1998).
4. Curtis, L. J., J. Phys. B **33**, L259 (2000).
5. Curtis, L. J., Ellis, D. G., Matulioniene, R. and Brage, T., Physica Scripta **56**, 240 (1997).
6. Curtis, L. J., Physica Scripta **62**, 31 (2000).
7. Condon, E. U. and Shortley, G. H., "The Theory of Atomic Spectra", (Univ. Press, Cambridge, 1935), [Footnote, pp. 273–4].
8. Wolfe, H. C., Phys. Rev. **41**, 443 (1932).
9. King, G. W. and Van Vleck, J. H., Phys. Rev. **56**, 464 (1939).
10. Curtis, L. J., Phys. Rev. A **40**, 6958 (1989).
11. Brown, C. M., Tilford, S. G. and Ginter, M., J. Opt. Soc. Am. **67**, 607 (1977).
12. Moore, C. E., "Atomic Energy Levels", Vol II, NSRDS-NBS 35 (US Govt. Printing Office, Washington DC, 1952 (Reissued 1971)).
13. Arcimowicz, B., Joshi, Y. N. and Kaufman, V., Can. J. Phys. **67**, 572 (1989).
14. Crooker, A. M. and Joshi, Y. N., J. Opt. Soc. Am. **54**, 553 (1964).
15. Tauheed, A., Joshi, Y. N. and Kaufman, V., J. Phys. B **24**, 3701 (1991).
16. Pinnington, E. H., Gosselin, R. N., Ji, Q., Kernahan, J. A. and Guo, B., Physica Scripta **46**, 40 (1992).
17. Tauheed, A., Joshi, Y. N. and Kaufman, V., Physica Scripta **44**, 579 (1991).
18. Bieroń, J. R., Marcinek, R. and Migdałek, J. Phys. B **24**, 31 (1991).
19. Lotrian, J., Cariou, J. and Johannin-Gilles, A., J. Quant. Spectrosc. Radiat. Transfer **16**, 315 (1976).
20. Corliss, C. H. and Bozman, W. R., "Experimental Transition Probabilities for Spectral Lines of Seventy Elements", NBS Monograph 53, US Govt. Printing Office, Washington DC, 1962.
21. Meggers, W. F., Corliss, C. H. and Scribner, B. F., "Tables of Spectral Line Intensities Part I – Arranged by Elements", NBS Monograph 145, US Govt. Printing Office, Washington DC, 1975.

